Tellus (1982) *34*, 39–49

Stability properties of mean flows with turning

By RICHARD GROTJAHN,[1] *National Center for Atmospheric Research,[2] P.O. Box 3000, Boulder, CO 80307, USA.*

(Manuscript received May 20, 1981)

ABSTRACT

The linear properties of eddies evolving in a mean flow that has backing or veering with height are analyzed. Several rates of turning are considered; the results for a 45° difference between the surface and upper level wind directions are illustrative and discussed in detail. The net compass orientation of the wind speed is also varied yielding results cognate with a previous article. Though the root mean square wind speed is unchanged, turning can significantly increase the growth rates since the *sum* of the two components of the vertical shear may be increased. The fastest growing wave has its wavefront aligned approximately perpendicular to the direction of the *upper* level flow. The wave properties are most easily influenced by the mean flow that is orthogonal to its wavefront. Thus waves moving parallel to the slow low-level flow propagate slower and are more bottom trapped than the waves moving with the faster upper flow. When there is turning, the relative importance of the variable Coriolis parameter is diminished.

1. Introduction

Travelling mid-latitude atmospheric cyclones are observed to grow in complicated flow fields. It is common practice to visualize these short-wavelength cyclones as being imbedded in an environment which, at least locally, can be ascribed to a baroclinic long wave. Because the long wave often has a westward tilt with height, the wind field in the vicinity of the cyclone will have turning with height, as well as (often) nonzonal average direction, curvature, vertical and horizontal shear and other varying properties. In an earlier paper (Grotjahn, 1981) the stability properties of eddies were examined for horizontally uniform mean flows oriented in any compass direction. In this article the stability properties are examined when turning of the mean wind with height is allowed as well. Investigations of curvature and other three-dimensional variations in the mean flow will be reported upon in the near future.

In an attempt to model the mid-tropospheric cyclones observed during the summer monsoon, Mak (1975) and Brode and Mak (1978) examined the linear stability properties of plane waves imbedded in two mean flows that turned with height. This report will refer to their work, but it is focused upon mid-latitude cyclones. The difference in emphasis leads to differing prescribed basic states that cause significant alterations in the properties of the solutions. This is particularly noteworthy for the assumed profiles of velocity. The model employed here is mathematically similar to theirs; the major difference is that the Coriolis parameter is not constant, but is allowed to vary linearly here. Using this "β-plane" approximation, Grotjahn (1981) found that the variation of the Coriolis parameter can greatly change some properties of the solutions. The relative importance of the β and the turning effects will also be addressed in this article.

2. Model

The model used in this study is derived from the model detailed in Grotjahn (1981) and its references. For completeness a brief description of the model follows, with emphasis placed upon those modifications made for the current usage.

[1] Present affiliation: Department of Land, Air and Water Resources, University of California, Davis, California 95616, U.S.A.

[2] The National Center for Atmospheric Research is sponsored by the National Science Foundation.

 0040-2826/82/010039-11$02.50/0

The motion of the fluid is constrained to conserve quasi-geostrophic potential vorticity. Periodic boundary conditions are used on the mid-latitude β-plane. The vertical velocity vanishes at the top and bottom boundaries. The equations are linearized and non-dimensionalized about a basic state. The vertical coordinate is height, z. (The Appendix contains a list of symbols.) The upper boundary condition is placed at a high enough altitude (50 km) to minimize its influence upon the solution. The horizontal coordinate axis x is aligned along the orientation angle γ, the orthogonal y axis is oriented as shown in Fig. 1.

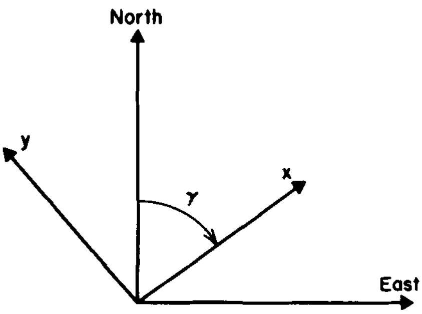

Fig. 1. Schematic illustration of the horizontal coordinate axes x and y for the orientation angle γ.

The orientation angle is measured positive clockwise from the poleward direction. The horizontal distances are scaled by the deformation length L ($\approx$1100 km); z is scaled by D = 10 km.

Most of the turning of the wind observed in mid-latitudes occurs in the lower portion of the atmosphere. To model this feature, the following expressions are employed for the two components of the mean flow U and V:

$$T_y = \Lambda(\tanh(\Xi z) + \tanh(\Xi \tau)), \quad T_x = (1 - T_y T_y)^{1/2}, \tag{1}$$

$$U(z) = T_x \bar{U}(z), \tag{2a}$$

$$V(z) = T_y \bar{U}(z) \tag{2b}$$

and

$$\bar{U}(z) = 1.8 \,|\, 1.0 - \tanh^2(1.0z) - \nu \exp(-0.1z)|$$

where $\nu = 1.0 - \tanh^2(1.0)$. Recall that $z = 1.0$ is a dimensional height of 10 km. $\bar{U}(z)$ is shown in Fig. 2; it is the same in all the experiments. Hence, the root mean square of U and V is the same in all the experiments. For the 45° turning experiments: $\Lambda = \pm 0.707$, $\tau = 0$, and $\Xi = 2.5$, making the rate of turning most rapid at the bottom surface and the mean flow almost unidirectional above 5 km. The surface mean flow is nearly directed at the angle γ in this case. When $\Lambda = 0.707$ the high altitude direction is $\gamma - 45$; when $\Lambda = -0.707$ the high altitude direction is $\gamma + 45$. In a 90° case ($\Lambda = 1.415$, $\tau = -0.25$, $\Xi = 2.2$), the surface flow orientation is $\gamma + 45°$ and the high altitude flow orientation is $\gamma - 45°$.

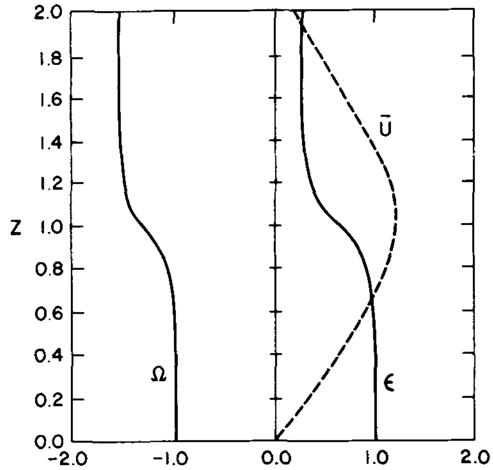

Fig. 2. Vertical profiles of ε, Λ and $\bar{U}$ used in the experiments.

The quasi-geostrophic potential vorticity, q is expressed as:

$$q = \varepsilon \Phi_{zz} + (\Omega \varepsilon + \varepsilon_z)\,\Phi_z + \Phi_{yy} + \Phi_{xx} \tag{3}$$

where subscripts denote differentiation and Φ is pressure. The Ω term is due to the compressibility of the fluid; it vanishes for incompressible flow. The coefficient ε is inversely proportional to the static stability, κ whose variation between typical tropospheric and stratospheric values is approximated by the relation

$$\varepsilon = \frac{f_0^2 L^2}{g \kappa D} = 0.70 - 0.35 \tanh(5.0(z - 1.0))$$

Profiles of these coefficients are also presented in Fig. 2.

The horizontal gradient of mean flow potential vorticity includes the planetary vorticity gradient β.

Its components may be expressed as:

$$\bar{q}_x = \varepsilon V_{zz} + (\Omega\varepsilon + \varepsilon_z)\, V_z + \beta \cos \gamma \tag{4a}$$

and

$$\bar{q}_y = -\varepsilon U_{zz} - (\Omega\varepsilon + \varepsilon_z)\, U_z + \beta \sin \gamma. \tag{4b}$$

Let the solutions be of the form

$$\Phi = \phi(z) \exp[i(kx + my - \omega t)]$$

and let $m = rk$ where r is a finite constant. These plane wave solutions are chosen in order to make the eigenvalue problem separable. For $r = -1.0$ the wavefront is oriented perpendicular to the angle $\gamma + 45°$; for $r = 0$ the wavefront is perpendicular to γ. It is clear from (4) and (5) that rotating the coordinate axes by angle γ will cause only the β terms to vary in the equations.

The linear conservation of the potential vorticity equation can be written

$$(-i\omega + ik\bar{V})(\varepsilon\phi_{zz} + (\Omega\varepsilon + \varepsilon_z)\phi_z - \alpha^2 \phi) + ik\phi\bar{Q} = 0 \tag{5a}$$

where

$$\bar{V} = U + rV,$$

$$\bar{Q} = \bar{q}_y - r\bar{q}_x$$

and $\alpha^2 = m^2 + k^2$ is the square of the absolute wavenumber of the plane wave. The vertical boundary conditions are derived from the adiabatic equation; they are

$$(-i\omega + ik\bar{V})\phi_z - ik\phi\bar{V}_z = 0$$

at $z = 0$ and 5.0, where

$$\bar{V}_z = U_z + rV_z.$$

Written in this way, these equations appear similar to those examined in many previous studies (e.g., Grotjahn, 1980). Indeed useful analogies can be drawn with some conclusions obtained by previous investigators. Compared with earlier work that considered zonal basic currents, $\bar{V}$ and $\bar{V}_z$ play the roles of the zonal current speed and its shear, while $\bar{Q}$ plays a consonant role as did the meridional gradient of basic state (including planetary) potential vorticity. However, the overbarred quantities now have very special definitions, and they are not as simply related as in that antecedent work. $\bar{V}$ and $\bar{V}_z$ are *weighted sums* of the two components of mean flow velocity and its vertical shear. $\bar{Q}$ is a *weighted subtraction* of the components of the basic state potential vorticity gradient. Different values of r only changed α in the earlier studies. Now $\bar{V}$, $\bar{V}_z$ and $\bar{Q}$ are altered as well. That is, the earlier work gave the same vertical structure, $\phi(z)$ when any combination of m and k (with $k \neq 0$) gave the same α. (For example, $m = k = \sqrt{2}$ and $m = 0$, $k = 2$.) Such simple correspondence no longer holds. The significance of these changes will become evident in the next section.

In Fig. 3, vertical profiles of $\bar{V}_z$ and $\bar{Q}$ are plotted for the 45 and 90° turning cases discussed later. In the figure $\gamma = 90°$ and $r = 0$ or 1. The magnitude of $\bar{V}_z$ is generally increased by greater turning of the mean flow. The mid-tropospheric maximum in $\bar{V}_z$ is greater when the wavefront is aligned more orthogonal to the flow there (as when $r = 1$) than when it is not (for $r = 0$). In one sense $\bar{V}_z$ is thus a measure of the mean shear *available* to plane waves with a particular value of r. The

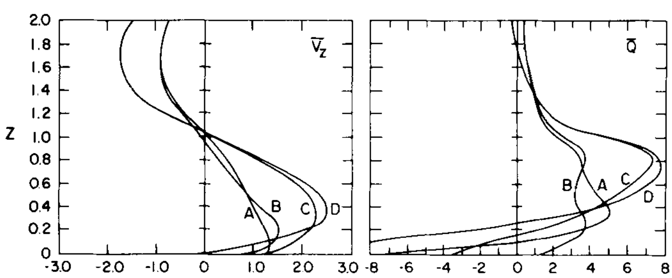

Fig. 3. Vertical profiles of $\bar{V}_z$ and $\bar{Q}$ for four cases. Case A is $r = 0$ and 90° turning of the mean wind with height. Case B is $r = 0$ and 45° turning. Case C is $r = 1$ and 45° turning. Case D is $r = 1$ and 90° turning. The 45° turning is $\Lambda = 0.707$, $\tau = 0$ and $\Xi = 2.5$; the 90° turning is $\Lambda = 1.415$, $\tau = -0.25$ and $\Xi = 2.2$.

$\bar{Q}$ profiles have a positive maximum somewhere in the troposphere. For the $r = 1$ waves aligned with the upper level flow, this maximum is at a high altitude. For the $r = 0$ waves the $\bar{Q}$ maximum is much lower. The choice of parameters in the 90° turning case causes the very large negative values of $\bar{Q}$ near the bottom. The wind turns most rapidly there. As with $\bar{V}_z$, these $\bar{Q}$ profiles display the amount of the gradient of mean potential vorticity available to the wave as a function of r.

The separable eigenvalue problem (5) is solved for ω and $\phi(z)$ by finite differencing the vertical derivatives and utilizing a highly accurate matrix eigenvalue routine. Typically, 41 levels were used in the vertical, though the solutions were little changed when more than 20 levels were used. A stretched vertical grid was used with the highest resolution near the bottom surface.

3. Results

The stability, motion and structure of the plane-wave solutions are described in this section. The results are presented in terms of α, the absolute wavenumber; the dimensional wavelength for $\alpha = 2.0$ is about 4500 km. The waves for $1.5 \leq \alpha \leq 2.5$ are referred to as intermediate waves. Those solutions for larger and smaller α are labelled short- and long-wave solutions respectively. The model is not well suited for representing the long waves and those solutions will not be mentioned. Following Grotjahn (1980), the desired solutions are chosen by selecting the eigenfunctions with the largest growth rate. This procedure is satisfactory for the intermediate and short waves set forth below. The results are symmetric about $\gamma = 90°$ for positive and negative Λ. That is, the results for $\gamma = 135°$ and $\Lambda = 0.707$ are the same as those for $\gamma = 45°$ and $\Lambda = -0.707$ with the opposite sign for r.

Growth rate spectra for the 45° turning case are presented in Fig. 4 for three values of r. When $r = 1$ in this case, the wavefront is perpendicular to the direction of the mean flow above about 5 km. This wave propagates in the direction parallel to that high altitude flow. The $r = 0$ wave is oriented orthogonal to the direction of the surface flow and propagates parallel to the x axis. Note that $\gamma = 90°$ means that the surface flow in this case is westerly, and the upper flow is southwesterly (since $\Lambda > 0$).

There are several characteristic features of the growth rate spectrum visible in Fig. 4. The growth rates vary significantly with the angle of orientation of the coordinate axes (and hence the direction of the mean flow). The variation with γ is not as great for the 45° turning case as it is when

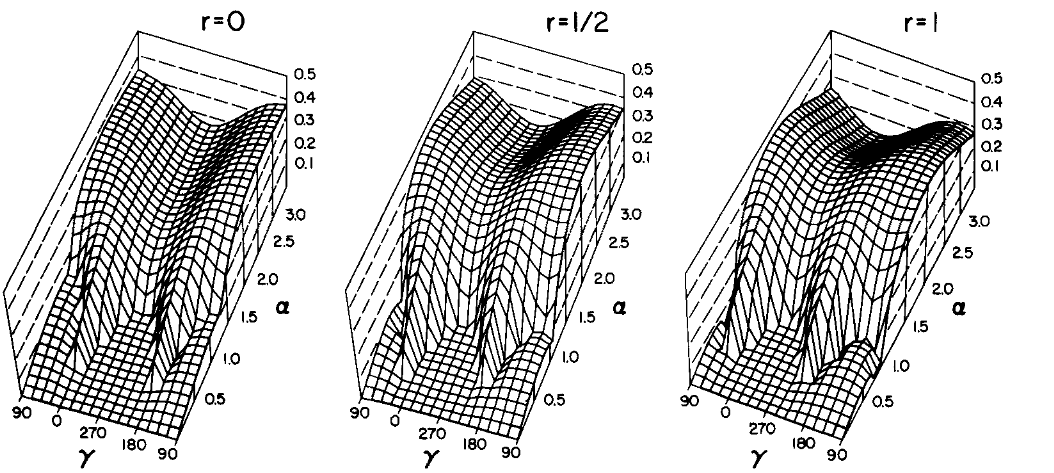

Fig. 4. Growth rate spectra versus α and γ for the 45° turning case, where $r = 0$ (left plot), $r = 0.5$ (middle plot) or $r = 1$ (right plot). The $r = 1$ plane waves move with the direction of the high altitude flow ($\gamma - 45°$).

no turning is present. And, when the mean wind turns through 90°, the variation is lesser still. This can be seen by comparing this figure with Fig. 3 in Grotjahn (1981). Recall that only the β-terms in $\bar{Q}$ change for different γ. Thus, this result reflects the diminishing relative importance of the β-terms in $\bar{Q}$ as the amount of turning is increased. Fig. 3 illustrates this. This fact also implies that the growth rates obtained by Brode and Mak (1978) might not be altered greatly if they included β, since the mean wind in their model turns very rapidly with height. Yet, the β-terms are still quite important for the amount of turning studied here. The wavelength of maximum instability shifts to slightly shorter wavelengths as the amount of turning increases. When there is no turning the most unstable wave generally propagates parallel to the flow. In Fig. 4, the largest growth rates occur for the $m = k$ plane wave, which moves in the direction of the upper level flow. Plane waves that move more in the *mean* direction of the basic flow (e.g., $r = 0.5$) have smaller growth rates than those that move more in the direction of the upper flow. In the 90° turning case this is still approximately true. The most unstable wave at $\alpha = 2.0$ has a value of $r \simeq 0.8$; this wave propagates nearly in the direction of the upper level flow. In cases where there is even stronger turning through a greater depth of the fluid (such as in Brode and Mak, 1978), the most unstable wave orientation will depend more upon the specific profiles of U and V. The most unstable wave for $r = 0$ has a much shorter wavelength than in the $r = 1$ case. In fact, the decay of the growth rate with wavelength is less for $r = 0$ than for $r = 1$ to such an extent that many of the short waves have larger growth rates for $r = 0$. This feature seems related to the structure of the eddies. The short waves are more bottom-trapped than the intermediate waves, so they respond primarily to the low level flow. The $r = 0$ short wave moves more nearly in the direction of the low flow than does the $r = 1$ short wave, and thereby more effectively feeds upon the mean flow vertical shear.

These effects are illustrated by Tables 1 and 2. Table 1 lists the largest growth rates found at four different values of γ, with the corresponding wavenumber indicated in parentheses. Table 2 lists selected growth rates at $\alpha = 3.0$. Both tables include the cases of 0, 45 and 90° turning of the mean wind with height. The tables show that the

Table 1. *Growth rate of most unstable wave (its wavenumber indicated in parentheses)*

	Case 1 no turning	Case 2 45° turning		Case 3 90° turning	
	$r = 0$	$r = 0$	$r = 1$	$r = 0$	$r = 1$
$\gamma = 45°$	0.456	0.361	0.449	0.428	0.482
	(2.0)	(2.3)	(1.8)	(2.5)	(1.9)
$\gamma = 90°$	0.460	0.371	0.470	0.437	0.499
	(2.0)	(2.5)	(2.0)	(2.6)	(2.0)
$\gamma = 135°$	0.456	0.361	0.473	0.428	0.498
	(2.0)	(2.3)	(2.1)	(2.5)	(2.1)
$\gamma = 270°$	0.354	0.197	0.397	0.297	0.435
	(1.9)	(2.1)	(1.9)	(2.7)	(1.9)

Table 2. *Growth rates for $\alpha = 3.0$. Growth rates for three types of mean flow at four orientations of the* high level *flow. The mean flow backs with height in these turning cases (i.e. westerly flow aloft means north westerly flow at surface for Type 2). In Types 2 and 3 the $r = 1$ waves move parallel to the upper flow. For veering of the flow, the results transpose about the case of westerly flow aloft*

Upper level flow from ↓	Type 1 no turning	Type 2 45° turning		Type 3 90° turning	
	$r = 0$	$r = 0$	$r = 1$	$r = 0$	$r = 1$
South West	0.3245	0.3561	0.3396	0.4277	0.3587
West	0.3472	0.3385	0.3580	0.4145	0.3705
North West	0.3245	0.2835	0.3396	0.3733	0.3587
East	0.1704	0.2110	0.2083	0.3192	0.2651

growth rates are increasing as the amount of turning becomes greater, and that the amount of the increase is proportionally greater for the short waves. Presumably, this is related to the increase in $\bar{V}_z$, which represents a net vertical shear of the basic current available for use by the wave.

The absolute phase speed is plotted in Fig. 5 for the waves presented in the previous figure. The absolute phase speed is the speed that the plane wave moves in the direction perpendicular to its wavefront. As with the growth rates, varying γ does not have as large an effect upon the phase speed when there is turning as it does when the flow is unidirectional. For a given α, that angle γ at which the wave grows the fastest is that angle where it moves the slowest, and vice versa. The

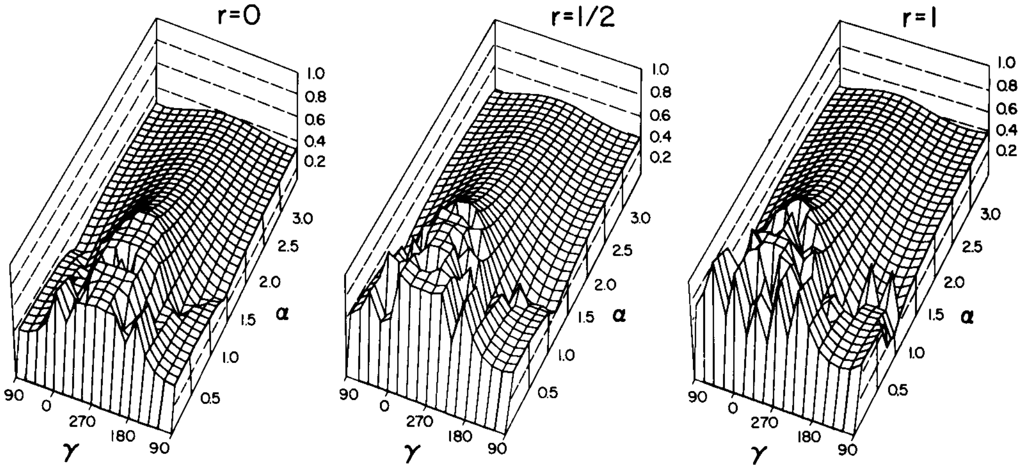

Fig. 5. Absolute phase speed spectra for the plane waves presented in Fig. 4.

$r = 1$ waves tend to propagate more rapidly than the $r = 0$ waves. This does not seem terribly surprising. The high altitude mean flow is faster than the low level flow and $r = 1$ waves respond more to the former while $r = 0$ waves respond more to the latter. This point is further verified by the structures adopted by the waves.

The vertical structure of some representative intermediate wavelength solutions are shown in Fig. 6. Fig. 7 shows the corresponding solutions for a short-wave mode. A mathematical symmetry in the solution is revealed by the schematic hodograms to the right of the graphs. The compass orientation convention is the same as that in Fig. 1. The short arrow shows the direction of the near surface flow, the long arrow represents the upper flow. Equivalent $r = 0$ solutions are aligned with the surface flows indicated. The $|r| = 1$ solutions aligned with their respective upper flows are also equivalent. The structure is depicted in terms of the eigenfunction amplitude and phase. The eigenfunction is specified by the problem up to an arbitrary complex constant. This constant is chosen such that the amplitude equals one and the phase angle equals zero at the bottom.

The intermediate waves have two relative maxima in their amplitude. The lower surface maximum is fixed by the normalization, while the upper maximum is near $z = 0.8$. In the antecedent study (Grotjahn, 1981), the upper maximum seemed to be linked in position and strength to the maximum in $\bar{q}_y$. An analogous correspondence, judging by the $\bar{Q}$ profiles in Fig. 3, is now less evident. The waves oriented orthogonal to the upper flow still show an apparent correspondence between eddy amplitude and the $\bar{Q}$ profiles. For the easterly type flows, that upper maximum is less than for westerly flows, as is $\bar{Q}$. But for the $r = 0$ waves, Fig. 3 shows two almost equal maxima in $\bar{Q}$, one near $z = 0.8$ and the other near $z = 0.3$. This lower maximum in $\bar{Q}$ is near where the eddy amplitude has a relative minimum in all the cases examined. A similar amplitude minimum even occurs in the 90° turning case when $r = 0$, a case where $\bar{Q}$ has one maximum near $z = 0.4$. The upper amplitude maximum, for the cases labelled B and C in Fig. 3, has almost the same magnitude and height. But the low relative minimum in wave amplitude occurs at $z = 0.2$ in case B and $z = 0.35$ for case C. The higher values of $\bar{Q}$ at low

Fig. 6. Vertical profiles of the eddy pressure amplitude (A) and phase angle (P) along with the baroclinic energy conversion (E) for the 45° turning case. These $\alpha = 2.0$ solutions are indicative of the intermediate waves. The directions of the near surface (short arrow) and upper level (long arrow) flow are depicted schematically to the right of each pair of graphs. The $r = 0$ modes propagate in the direction of the short arrows; the $|r| = 1$ modes are those waves which propagate parallel to the long arrows. A mathematical symmetry in the problem gives the same result for a pair of mean flow orientations.

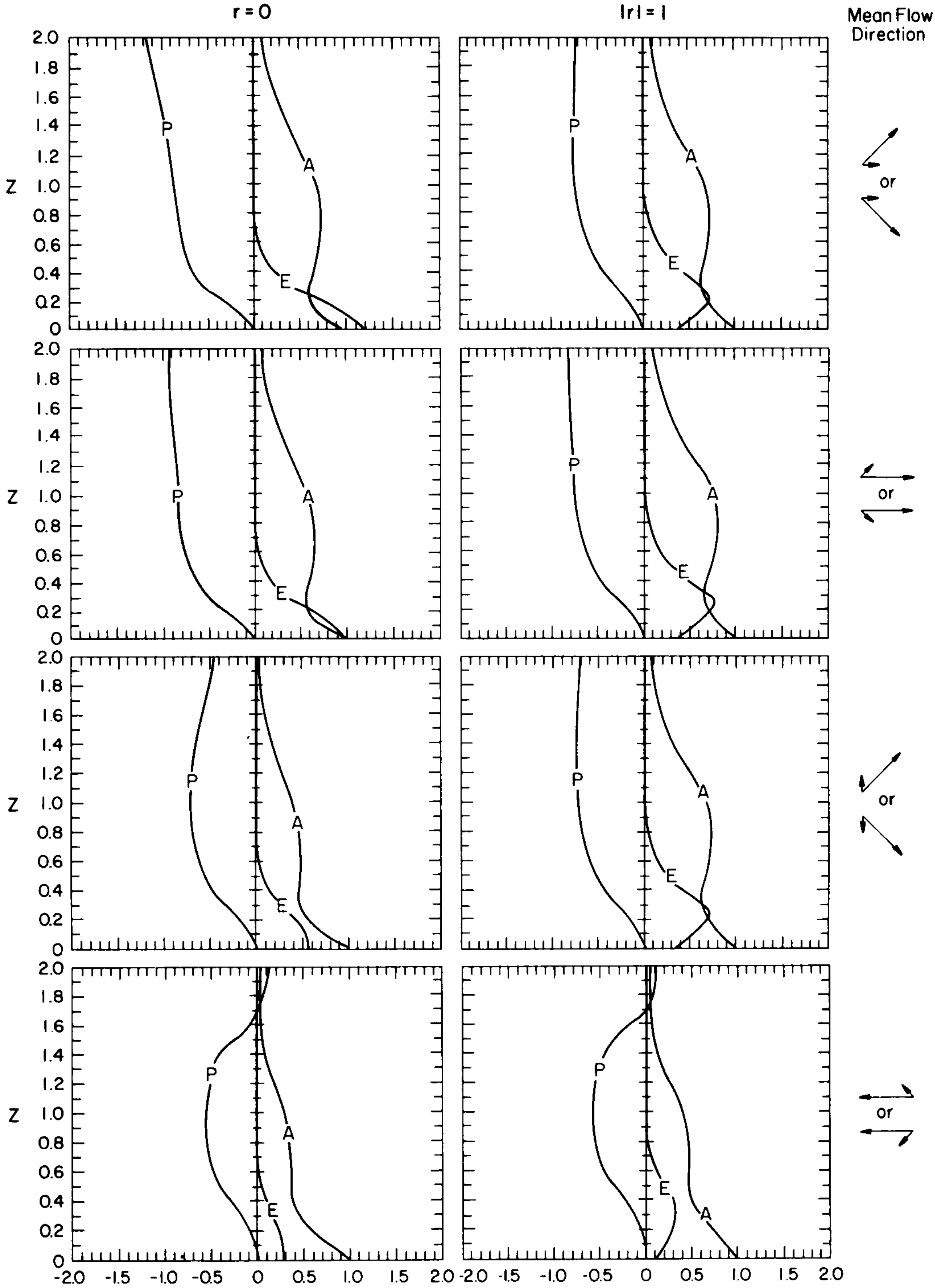
r = 0
|r| = 1
Mean Flow Direction
or
or
or
or
Z
P
A
E
2.0
1.8
1.6
1.4
1.2
1.0
0.8
0.6
0.4
0.2
0
-2.0 -1.5 -1.0 -0.5 0 0.5 1.0 1.5 2.0

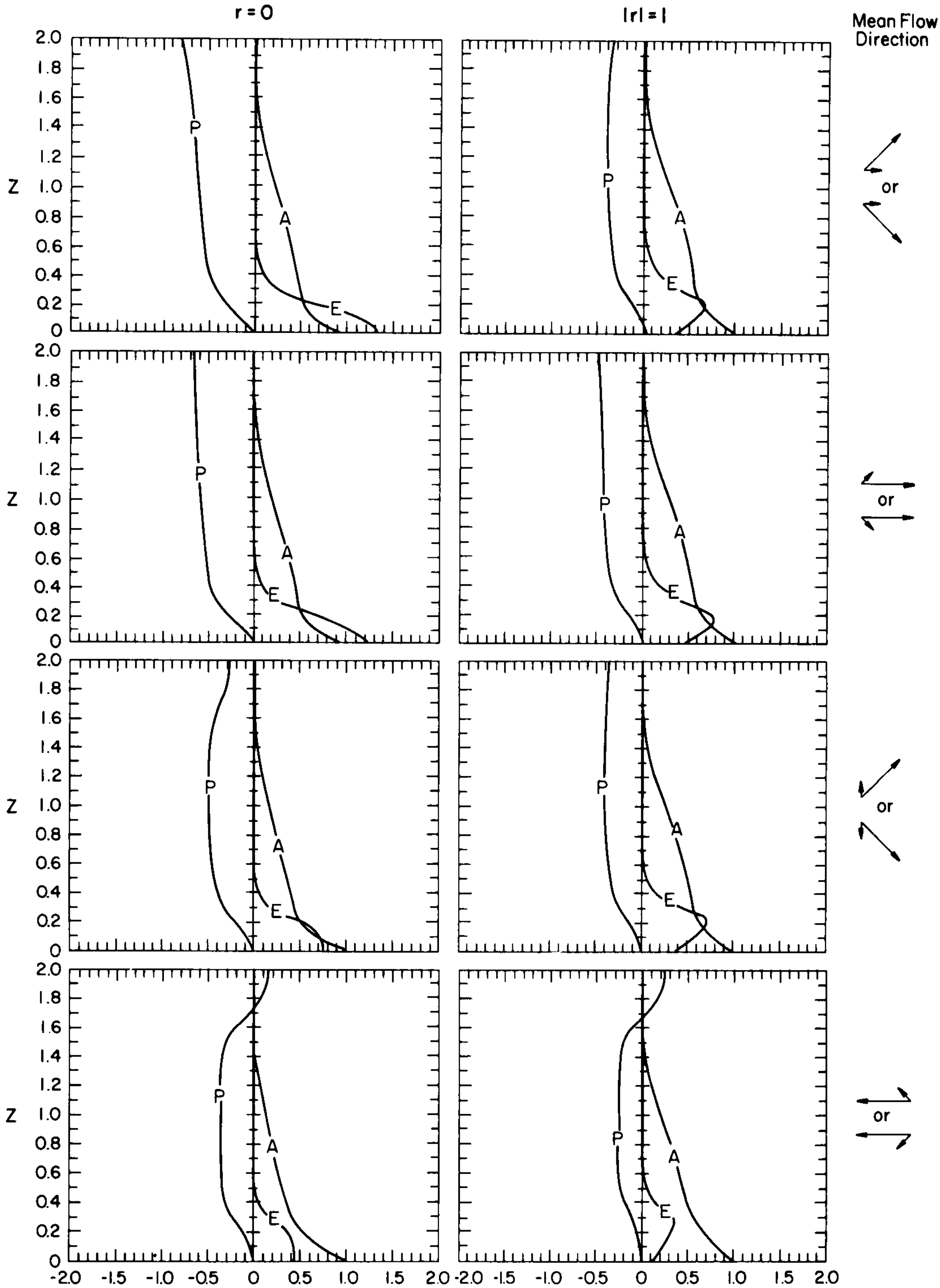

Fig. 7. Same as Fig. 6 except for the short waves $\alpha = 3.0$.

levels seem to increase the amplitude locally and thereby lower the level of the eddy amplitude minimum. Similar statements hold for the short-wave solutions shown in Fig. 7. The differences between the various cases are less apparent for the short waves because they are more bottom-trapped than the intermediate waves.

The double maxima in the amplitude profile seem to be a persistent feature of this type of study. Brode and Mak (1978) used a mean wind profile with very strong turning and by inspection it is clear that $\bar{Q}$ for their study would look quite different from any of the profiles shown in Fig. 3. Yet their most unstable solutions still exhibit a double maximum, one at the bottom surface, the other at an interior level whose altitude is influenced by the wavenumber, static stability and other parameters.

There is much theoretical and experimental experience indicating that $\bar{Q}$ should have a key influence upon the wave properties. After all, the system of equations (5) is expressible as conservation of quasi-geostrophic potential vorticity (Bretherton, 1966), and the eddy advection of $\bar{Q}$ provides the forcing for the eddy potential vorticity, q' advected by the mean flow. The eddy pressure is mathematically linked to q' via the Poisson operation (3), hence it tends to be smoother than q' and therefore smoother than $\bar{Q}$, given a reasonably smooth $\bar{V}$ profile. Some very general comments can be made, but the precise modification of the wave structure by $\bar{Q}$ and $\bar{V}$ seems equivocal. In the antecedent study, the connection appeared more straightforward; it now seems as if that may have been a fortuitous consequence of the simplicity of that problem. This is perhaps disappointing, but not really surprising. Previous work has shown that a $\bar{Q}$ profile which changes sign in the domain provides an assurance that instability is possible; further, the $\bar{Q}$ profile can be used to determine a range for the complex phase speed. Examples are found in Pedlosky (1964) and Lindzen *et al.* (1980). But a more precise estimate requires at least some explicit calculation. On the other hand, the lack of a strong correlation between the profiles of $\bar{Q}$ and wave amplitude can be beneficial. Since $\bar{Q}$ contains first and second order derivatives of the velocity, small changes in the profiles of U and V can radically alter $\bar{Q}$ as one can see in Fig. 3. One would not expect to derive radical changes in the wave structure for small changes in the ambient wind field because that is not observed. Indeed this moderation in the wave response will be advantageously employed in a forthcoming study of three-dimensional basic flows.

Vertical profiles of the phase angle of the plane waves are also presented in Figs. 6 and 7. The convention used is that negative values show upstream displacement, relative to the direction of wave propagation. (The angle in radians is divided by two in these figures.) The waves tilt upstream with height. The greatest tilt is generally where the amplitude profile has its lower level relative minimum. The strongest tilt thereby occurs at a lower height for the more bottom trapped $r = 0$ waves than for the $r = 1$ waves. The upstream tilt is stronger for the waves with the larger growth rates. One would expect such behavior since stronger tilt implies greater baroclinic energy conversion up to a point, and that conversion is proportional to the growth rate. For waves imbedded in flows with an easterly nature, there is a westerly tilt above the "tropopause" level ($z = 1.0$).

Figs. 6 and 7 also include profiles of the baroclinic energy conversion. This is the source of energy for these waves since the mean flow has no horizontal shear. The energy conversion is indeed larger for the westerly flows, which have greater growth rates, than for the easterly flows. The growth rate can be independently estimated by taking the volume-integrated average of the energy conversion and dividing by the volume-integrated total eddy energy. This calculation was performed and agreed with the growth rates derived from the eigenvalues to within at least three significant digits. The energy conversion for the ($r = 0$) waves orthogonal to the near bottom flow is largest at the bottom, while it is largest around $z = 0.25$ for the ($|r| = 1$) waves orthogonal to the high level flow. This result was commented upon in the amplitude and phase angle and is more noticeable for the energy conversion. If one chooses a wavefront oriented even more parallel with the low level flow, such as $r = 2$ for $\Lambda > 0$, then this effect is enhanced further. The level of maximum baroclinic energy conversion is slightly higher for easterly flows compared with westerly flows; this is discussed by Grotjahn (1981). This results from the changing values of the β terms in $\bar{Q}$. Hence, the effect of different orientations of the mean flow is not as pronounced here as it was in the antecedent study.

4. Conclusions

This article discussed the linear properties of plane waves immersed in a mean flow that has backing or veering with height in the lowest 5 km. The cases where there is a 45° angle between the near surface flow and the high altitude flow were detailed. The solutions where $r = 0$ have wavefronts approximately perpendicular to the bottom flow direction. The $|r| = 1$ solutions are oriented orthogonal to the upper flow direction.

The most unstable wave tended to be oriented orthogonal to the upper flow for this type of turning. Westerly flows tended to be more unstable than easterly flows. The most unstable mode (varying only γ) tended to be the slowest propagating and vice versa. The amplitude profile of the intermediate waves was characterized by maxima at the surface and near $z = 0.8$. The relative minimum in between is where the upstream tilt with height of the waves was greatest. As α increased, the (shorter) waves became more bottom trapped.

The wave was most easily influenced by the mean flow that is parallel to its direction of propagation. (That is, perpendicular to its wavefront.) Thus the $r = 0$ waves were more bottom trapped: the upper amplitude maximum was less and the greatest upstream tilt with height occurred at a lower level than for the $|r| = 1$ waves. The baroclinic energy conversion was largest at the bottom for the $r = 0$ waves; it was largest near $z = 0.25$ for the $|r| = 1$ waves. The near surface flow orthogonal to the $r = 0$ wavefront was weak and existed in a shallow layer because the turning was rapid there. So, the growth rates and phase speeds of the $r = 0$ intermediate waves were usually less than those for the $|r| = 1$ waves. Also, the most unstable wave for $r = 0$ had a shorter wavelength than for $|r| = 1$. For α greater than some short wavelength value, the $r = 0$ short waves were destabilized to such an extent that they grew more rapidly than the corresponding $|r| = 1$ short waves. In other words, this linear study suggests that intermediate waves would tend to move in the direction of the high-level flow and short waves move more in the direction of the low-level flow when there is low-level turning. (It is implicitly assumed that the most unstable wave for a given α would be dominant.)

Those effects attributable to the variation of γ agreed with the results found by Grotjahn (1981). Varying γ changed the β terms in $\bar{Q}$ which arise from the variation of the Coriolis parameter. However, those effects were diminished when there was strong turning because the β terms were dwarfed by the other terms in $\bar{Q}$. Since Brode and Mak (1978) used a basic wind profile with much stronger turning, their neglect of the β terms is not nearly as bad as it would be for unidirectional flow. Even so, variation of the β terms still causes significant changes in the wave properties (especially the growth rates).

In the antecedent study (Grotjahn, 1981) it was suggested that the upper level maximum in the wave amplitude was directly linked to the maximum in the $\bar{Q}$ profile near the same height. It was indicated here that the correlation may have been rather fortuitous. Instead, the wave structure changed in modest ways for the different cases examined, despite wildly different $\bar{Q}$ profiles. This was due in part to the properties of the Poisson operation which linked the pressure and its potential vorticity fields. The changes were more moderate for the pressure field than for its derivative fields of temperature and velocity. Still, these latter fields did not exhibit such extreme fluctuations as did $\bar{Q}$.

5. Appendix

D	Vertical length scale $[=10\ \text{km}]$
f_0	mean Coriolis parameter
g	acceleration of gravity
k	x direction wavenumber
L	Rossby radius of deformation at surface; horizontal length scale $[\sim 1100\ \text{km}]$
m	y direction wavenumber
$\bar{Q}$	available interior mean potential vorticity gradient $[=\bar{q}_y - r\bar{q}_x]$
$\bar{q}_x, \bar{q}_y$	x, y gradients of mean potential vorticity
r	wave aspect ratio $[m = rk]$
U, V	x, y components of mean flow
$\bar{V}$	net mean flow velocity $[=U + rV]$
$\bar{V}_z$	available mean flow vertical shear $[=U_z + rV_z]$
x, y	horizontal coordinates, see Fig. 1
z	vertical coordinate
α	absolute wavenumber $[=(k^2 + m^2)]$
β	first meridional derivation of f
γ	orientation angle clockwise from northward
ε	$[=f_0^2L^2/g\kappa D]$

θ_s horizontal mean potential temperature
κ static stability $[=D(\ln \theta_s)_z]$
Λ amount of turning parameter
Ξ rate of turning parameter
τ maximum rate of turning height
ϕ eddy pressure

REFERENCES

Bretherton, F. P. 1966. Critical layer instability in baroclinic flows. *Quart. J. Roy. Meteor. Soc. 92*, 325–334.

Brode, R. W. and Mak, M. 1978. On the mechanism of the monsoonal mid-tropospheric cyclone formation. *J. Atmos. Sci. 35*, 1473–1484.

Grotjahn, R. 1980. Linearized tropopause dynamics and cyclone development. *J. Atmos. Sci. 37*, 2396–2406.

Grotjahn, R. 1981. Stability properties of an arbitrarily oriented mean flow. *Tellus 33*, 188–200.

Lindzen, R. S., Farrell, B. and Tung, K.-K. 1980. The concept of wave-overreflection and its application to baroclinic instability. *J. Atmos. Sci. 37*, 44–63.

Mak, M. 1975. The monsoonal mid-tropospheric cyclogenesis. *J. Atmos. Sci. 32*, 2246–2253.

Pedlosky, J. 1964. The stability of currents in the atmosphere and ocean: Part 1. *J. Atmos. Sci. 21*, 201–219.